Slow and fast light in quantum-well and quantum-dot semiconductor optical amplifiers

Invited Paper

Piotr Konrad Kondratko, Akira Matsudaira, Shu-Wei Chang, and Shun Lien Chuang

Department of Electrical and Computer Engineering, University of Illinois at Urbana-Champaign, Urbana IL, 61801, USA

Received June 16, 2008

Slow and fast light in quantum-well (QW) and quantum-dot (QD) semiconductor optical amplifiers (SOAs) using nonlinear quantum optical effects are presented. We demonstrate electrical and optical controls of fast light using the coherent population oscillation (CPO) and four wave mixing (FWM) in the gain regime of QW SOAs. We then consider the dependence on the wavelength and modal gain of the pump in QW SOAs. To enhance the tunable photonic delay of a single QW SOA, we explore a serial cascade of multiple amplifiers. A model for the number of QW SOAs in series with variable optical attenuation is developed and matched to the experimental data. We demonstrate the scaling law and the bandwidth control by using the serial cascade of multiple QW SOAs. Experimentally, we achieve a phase change of 160° and a scaling factor of four at 1 GHz using the cascade of four QW SOAs. Finally, we investigate CPO and FWM slow and fast light of QD SOAs. The experiment shows that the bandwidth of the time delay as a function of the modulation frequency changes in the absorption and gain regimes due to the carrier-lifetime variation. The tunable phase shift in QD SOA is compared between the ground- and first excited-state transitions with different modal gains.

OCIS codes: 230.4320, 270.1670, 250.5980.
doi: 10.3788/COL20080610.0736.

1. Introduction

A compact, electrically and optically tunable optical buffer which operates at room temperature is one of the essential elements in the future optical communication system. An all optical buffer eliminates the need for electrical-to-optical and optical-to-electrical conversions of the transmitted signal. It can provide data storage to buffer optical signals during the traffic jam of information flow. These requirements stimulate the investigation of the slow and fast light. Since most of the slow- and fast-light phenomena are based on the dispersion and phase tuning from materials or designed spatial structures, they can also be applied to other areas such as dispersion compensation (pulse shaping) and the optical control of microwave antenna arrays.

There are several approaches to implement slow and fast light. The conventional one is to switch the signal pulse into a fiber loop[1]. This scheme can provide high bandwidth and multi-bit delay but requires physical switching of the signal into the fiber loop. Since the length of the fiber is fixed, the time delay is fixed. Thus, only discrete rather than continuous tuning is possible by using different lengths of fibers. The second type is based on the exotic quantum or nonlinear optical interactions between light and matter such as electromagnetically induced transparency (EIT) and coherent population oscillation (CPO)[2−4]. A large slowdown factor is the most spectacular feature of this approach. However, some examples in this category require extreme operation conditions such as low temperature or bulky experimental setup. Also, the bandwidth is limited by the corresponding dynamics of the system, and in many cases is too narrow to be used in real applications. The third type is to utilize the filter effect from the designed spatial structure such as ring resonators[5] or photonic-crystal waveguides[6]. This approach can provide the necessary tunability and bandwidth engineering. However, the shortcoming from dispersion still requires improvement.

For compact integration with active optoelectronic devices, it is desirable to implement optical buffers on semiconductors, which can also provide electrical and optical control of slow and fast light. The basic working principle of slow or fast light is to manipulate the group velocity of the wave packet by the engineering of linear dispersion or nonlinear propagation. An example for the first category which is commonly used in semiconductors is CPO, and an instance of the second type is the four wave mixing (FWM), which is usually accompanied with the presence of CPO. Compared with other control schemes, semiconductor slow-light devices can offer not only optical[7,8] but also electrical control based on the forward current injection or reverse voltage bias[9−16]. This feature makes the semiconductor unique among other slow- and fast-light schemes.

In this letter, we first discuss the fast light based on CPO and FWM in quantum wells (QWs). The experiments of electrical and optical control of the fast-light system are then presented with new data. Wavelength and modal gain dependences of the pump laser are observed and modeled. We show that our theoretical results agree very well with experiments. Furthermore, we demonstrate the scaling law by using cascaded QW semiconductor optical amplifiers (SOAs) operating above transparency. Finally, slow and fast light in quantum-dot (QD) SOAs are investigated using absorption and gain by changing the bias current.

2. Slow and fast light via CPO and FWM

Coherent population oscillation is the beating of the carrier density induced by an intense pump and probe signal. Usually, the pump is a continuous-wave (CW)

laser beam with a frequency close to the transition energies of the upper and lower states. In semiconductor nanostructures, such states can be the first conduction and heavy-hole (HH) valence subbands in QWs, or the ground conduction and valence states of QDs. The intense pump light saturates the absorption or gain of the material, depending on whether the device is biased in the absorption or gain regime. Suppose that the signal with a frequency detuning from the pump frequency is incident into the material. If the detuning is much larger than the inverse of the population lifetime, the induced population beating cannot follow the high-speed modulation and will have a small oscillation magnitude. In this case, the signal simply experiences the saturated gain and absorption. On the other hand, if the frequency detuning is small, the magnitude of the induced beating can be significant, and part of the signal energy can be converted into the population beating without being dissipated or amplified by the medium. Correspondingly, there will be an absorption or gain dips centered at the pump frequency on the absorption/gain spectrum. From the Kramers Kronig relation, a positive-slope (negative-slope) variation of the refractive-index spectra will accompany this absorption (gain) dip. The corresponding group velocity is inversely proportional to the group index $n_{\rm g}$, which is related to this slope:

$$v_{\rm g} = \frac{c}{n_{\rm g}} = \frac{c}{n + \omega \frac{\partial n}{\partial \omega}}, \quad (1)$$

where c is the vacuum speed of the light, n is the real part of the refractive index. In the absorption regime, the induced slope $\partial n/\partial\omega$ is positive (a larger group index $n_{\rm g}$), and thus slow light is obtained. In contrast, the negative slope in the gain regime (a smaller $n_{\rm g}$) leads to fast light. The above picture describes the linear response experienced by the signal. In addition, the induced population beating can also generate a conjugate signal via the nonlinear FWM. The effect of FWM is important in the gain regime and cannot be discarded.

For CPO and FWM based on semiconductor materials, there are two main effects which can influence the slow and fast light when the electrical current injection or reverse voltage bias is applied to the semiconductor nanostructure. One is the change of the electronic-state occupation, which affects the background gain or absorption. The other is the bias-dependent carrier dynamics, which changes the linear and nonlinear susceptibilities experienced by the signal. The former determines whether the signal experiences slowdown or speedup while both factors play a significant role on the amount of time delay, pulse broadening, and distortion.

Let us take a QD SOA as an example. Slow light is present in the reverse-bias regime and the small forward-bias regime before the zero modal gain is reached. Furthermore, the recombination lifetimes (carrier dynamics) in the forward and reverse bias regimes are different because in the reverse-bias regime, the carriers can be swept out of QDs by the applied electric field and thus lead to a shorter lifetime[11,13]. The shorter lifetime results in a broader bandwidth for the signal, but also less amount of time delay. On the other hand, the lifetime is pretty constant in the forward-bias regime before the transparency is reached, mainly due to a constant radiative lifetime. This indicates that different mechanisms corresponding to distinct carrier dynamics may be involved in the slow-light phenomena.

The even higher current injection into QDs above the transparency level brings the slow-light regime into the fast-light regime[15] as a result of the gain dip rather than absorption dip. However, in the gain regime, in addition to CPO, FWM also becomes important because both of the signal and generated conjugate can be amplified and converted to each other in the SOA. In general, for a sinusoidally-modulated signal, the phase shift, which is related to the amount of time advance in the fast-light regime, is influenced by CPO and FWM simultaneously, and their effects cannot be separated. In the gain regime, other nonradiative recombination mechanisms also come into play, which lead to a shorter carrier lifetime[15]. The faster carrier dynamics will again influence the amount of advance in the fast-light regime.

The slow and fast light in other systems such as QW or bulk SOAs follow similar mechanisms, but their different carrier dynamics can show distinct characteristics of slow and fast light. One of the key factors is the linewidth enhancement factor[17]. The linewidth enhancement factor can lead to skewed lineshape of the gain dip, and as a result, both slow and fast light can be observed based on CPO in the gain regime[18]. Note that the effect of the linewidth enhancement factor is not always present in the experiment. For example, in the phase-shift experiment of the sinusoidally-modulated signal, the phase advance of the modulated signal does not reflect the effect of the linewidth enhancement factor[19].

3. Slow and fast light experiment

Figure 1 shows the experimental setup used in the measurements of CPO and FWM slow and fast light in the SOA. A strong pump beam from the distributed-feedback (DFB) laser diode is modulated by an external modulator with a continuously variable radio frequency (RF) signal from a network analyzer. A modulated signal is coupled into the SOA by fiber lenses. The magnitude and the phase differences of RF modulated signal are measured by the network analyzer at different current injections into the SOA. An erbium-doped fiber amplifier (Amp) is inserted to preamplify the modulated input signal so that the signal in the absorption regime can be measured. The gain of this Amp is kept constant throughout the experiment. The experiment is performed at room

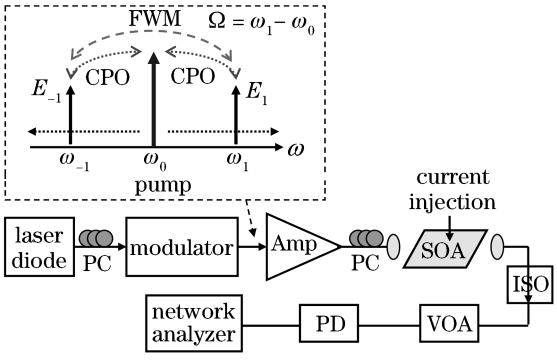

Fig. 1. Experimental setup used in measuring single modulated slow and fast light. VOA: variable optical attenuator; PD: photodetector; PC: polarization controller; ISO: isolator.

temperature.

A single microwave-modulated beam consists of a strong direct current (DC) pump beam (E_0) with two sidebands (E_1 and E_{-1}) separated by the modulation angular frequency Ω, as shown in the inset of Fig. 1. The optical frequency of the center pump beam (E_0) serves as the optical carrier frequency, and the sidebands carry the information from the sinusoidal envelope, which propagate with the group velocity.

We use the analytical solutions, Eqs. (3.17) and (3.18) in Ref. [20], which include CPO and FWM effects to model modal gain G (cm^{-1}) and phase delay $\Delta\phi$ of a sinusoidally-modulated probe signal propagating through an SOA in the gain or absorption regime (fast or slow light)[19,20]. Our solutions describe the spectral behavior of probe gain and phase (or time delay using relation of $\Delta\phi = \Delta t_{\mathrm{d}}\Omega$) analytically based on device modal gain Γg, carrier lifetime τ, intrinsic loss α_{int}, and length L. The input power P_{in} and output power P_{out} are normalized to device saturation power. These parameters are evaluated based on gain saturation characteristics according to the intensity of the traveling wave within the SOA[21] as follows:

$$(\Gamma g - \alpha_{\mathrm{int}})L = \ln\left(\frac{P_{\mathrm{out}}}{P_{\mathrm{in}}}\right) - \frac{\Gamma g}{\alpha_{\mathrm{int}}}\ln\left[\frac{\Gamma g - \alpha_{\mathrm{int}}(1+P_{\mathrm{out}})}{\Gamma g - \alpha_{\mathrm{int}}(1+P_{\mathrm{in}})}\right]. \quad (2)$$

4. Observation of fast light in QW SOA

The QW SOA in this experiment exhibits about 23−25 dB gain (at a maximum injection current of 500 mA) and is controlled by a DC controller biased at or above transparency. The SOA is 2-mm long and operates at 1.3 μm. To disregard and calibrate the contribution of propagation time through the QW SOAs, optical RF thru-calibration is performed when the device is near the transparency. The active medium near transparency achieves negligible CPO and FWM effects. The RF calibration at this current gives a zero-magnitude response, zero-phase response, and therefore no delay at transparency (the propagation delay is assumed constant with any increase of injection current).

In Fig. 2, we present experimental (symbols) gain (top) and phase (bottom) spectra for the modulated optical pump through an electrically controlled QW SOA. The theoretical calculations (lines) based on CPO/FWM theory[19,20] are shown to fit the experimental data very well. For all phase measurements, the measurement at 60 mA is used as a reference (zero modal gain within the device) and is indicated in the figure. With increasing current (gain), the phase becomes more negative and, therefore, the delay decreases. Relatively, this is equivalent to an optical advance or fast light as current is increased from 60 mA. A relative delay is achieved by decreasing the current from 460 mA to transparency. The relative delay of this system is frequency-dependent and can be evaluated by using $\tau_{\mathrm{d}} = \Delta\phi/(2\pi\Delta f)$. Table 1 shows parameters extracted from the experimental data of phase and magnitude. The carrier lifetime is found to reduce from about 0.4 to 0.18 ns. This is attributed to the increase of stimulated emission at a larger modal

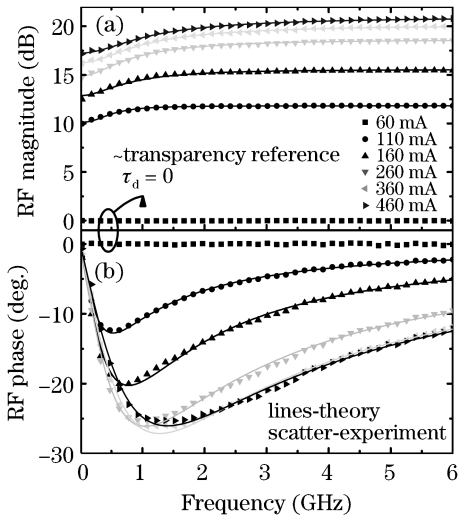

Fig. 2. RF gain relative to that at transparency and phase measurements for a variable optical delay line with a single QW SOA. Symbols: experiment. Curves: theory. (a) Optical RF magnitude spectra relative to that at transparency (60 mA) of the SOA medium. (b) RF phase spectra with increasing current injection relative to that at transparency. The increase in gain enhances CPO/FWM, giving a larger negative delay.

Table 1. QW SOA Parameters Extracted from Experimental Observations (Symbols) and Subsequently Used to Model the Spectra (Lines) in Fig.2. In the Model Fitting, the Length L is Fixed to 2 mm

Current (mA)	τ (ns)	Γg (cm^{-1})	α_{int} (cm^{-1})	$\frac{P_{\mathrm{in}}}{P_{\mathrm{sat}}}$
110	0.395	23.0	7.0	0.016
160	0.323	29.1	7.0	0.014
260	0.247	34.2	7.0	0.012
360	0.207	36.1	7.0	0.011
460	0.185	37.0	7.0	0.010

gain and therefore, shorter carrier lifetime. Moreover, the intrinsic absorption α_{int} is found to be 7 cm^{-1}.

The frequency-domain analysis is also correlated to the time-domain experiment. The traces of 1-GHz modulated pump at two bias currents are shown in Fig. 3. A direct correlation of the time-domain advance with the phase response of the single tone at 1 GHz is also

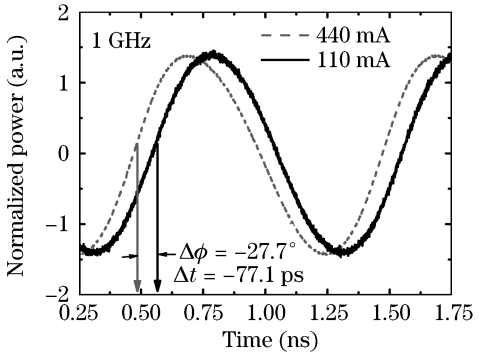

Fig. 3. Normalized time domain traces at 1 GHz modulation for 100 and 440 mA currents into the QW SOA. The optical advance (or negative delay) is observed with increasing bias current in the QW SOA.

performed (data not shown). The extraction of time delays from oscilloscope is obtained by cross-correlation analysis of all waveforms to transparency waveform. In the time-domain experiments, the same magnitude of phase change is observed, as shown in Fig. 2. Overall, about $-27.7°$ is observed in both measurements, and this corresponds to 77.1 ps advance from 100 to 440 mA (fast light).

5. Optical power control and wavelength dependance

The optical control by changing the pump input power to the QW SOA is investigated experimentally and modeled. Moreover, fast light by CPO/FWM is observed at different pump wavelengths across broad gain spectrum of the QW SOA. Optical pumps at different wavelengths experience different maximum modal gain. The fast-light effects at different pump wavelengths are modeled by varying maximum modal gain in the SOA.

The maximum phase shifts (relative to that at transparency with 1 GHz modulation) are plotted in Fig. 4. The phase shifts of the probe are plotted versus the normalized input pump power. Four wavelengths are used across the gain spectrum of the QW SOA (see top inset of Fig. 4). To facilitate experimental data acquisition, the measurements of the phase shift are taken at 1 GHz fixed modulation frequency. This measurement gives only the maximum phase change with the 1 GHz modulation and does not give overall highest relative phase change, which may occur at other modulation frequencies (see Fig. 2). The theoretical model of maximum phase change at 1 GHz modulation is also plotted (lines). Each theoretical line which is matched to experimental observation (scatter) differs only by the maximum modal gain in our theoretical model. To model the experimental data, we adopt $\Gamma g = 18$, 27, 22, 15 cm^{-1} at 1290, 1308, 1330, and 1350 nm, respectively. These parameters agree well with the spectral dependance of the gain. All other parameters are set to the values given in Table 1. The input power is swept from 0 to 1 (normalized). The DFB pump at 1308 nm is capable of large power output (> 6 mW or about half of saturation power) and enables the observation of maximum phase pinning and its subsequent reduction. The remaining pumps at different wavelengths (1290, 1330, and 1350 nm DFBs) with maximum output power of about 2 mW show decreased modal gains and, therefore, reduced maximum optical control of fast light.

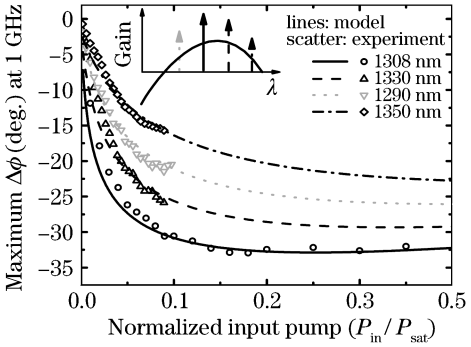

Fig. 4. Experimental (symbols) maximum relative phase change versus input pump power at different pump wavelengths. The change in input pump power (normalized to saturation power of the SOA) achieves variable optical control. Experimental data (symbols) using three low-power DFB lasers (at 1290, 1330, 1350 nm) and one high output power DFB pump at 1308 nm. The 1308 nm is able to saturate and reduce the maximum phase change. Theoretical model (solid lines) of maximum phase change at 1 GHz versus input pump power is also shown. Pump-wavelength dependence at different wavelengths is modeled using the maximum attainable modal gain and is illustrated in the top inset.

The effect of saturation and subsequent reduction in the maximum phase (pump at 1308 nm) is an interesting observation and is shown both experimentally and theoretically. This phenomenon is explained by the saturation of the propagating pump in the active medium and was previously modeled[11]. With an increase of the input pump power, the broadening of the modulation response in the frequency domain occurs, and the magnitude of the gain dip saturates (therefore, phase pins and broadens). With a further increase of the input power, the bandwidth is broadened, and the saturated spectral gain dip reduces in magnitude due to the larger signal power propagating within the medium. This occurs because the gain of the device decreases with a larger input power. This gain reduction causes the spectral CPO/FWM dip to be reduced and broadened. Phenomenologically, the spectral dip in gain due to CPO/FWM is first saturated in magnitude and broadened in frequency, and then decreases in magnitude as it further broadens in the frequency domain. With reduced maximum modal gain (at different pump wavelengths), the phase saturation and subsequent reduction of maximum phase change occurs at higher input pump powers. This is mainly attributed to the gain saturation of the SOA at a larger pump power for that particular wavelength. The observation is illustrated by theoretical curves at different wavelengths in Fig. 4.

So far, we presented experimental and theoretical analyses of the CPO/FWM in the electrically controlled QW SOA active medium. Tuning of the optical delay is achieved electrically by changing the background gain with electrical current injection or optically by changing the intensity of the input pump. Our study shows FWM/CPO experimental results using a single QW SOA with a delay of about 80 ps ($\sim 30°$) and a bandwidth exceeding 1 GHz. The experimental data in the time domain confirm the frequency-domain observations. The theoretical model predicted successfully the experimental results of the SOA modal gain and input power dependence of fast light. The delay-bandwidth product is found experimentally to be about 0.08.

6. Fast light in cascaded QW SOA

The CPO/FWM nonlinear interactions in a single QW SOA operating above gain transparency current (fast light) can be exploited to increase the delay-bandwidth product using the cascaded chain of QW SOAs. This scheme has the advantage that it always amplifies the incoming signal. First, we discuss a model for N cascade of SOAs, which is based on the probe gain and phase delay for a single QW SOA[19,20]. The model is presented for the delay-bandwidth dependence on N, the number of SOAs, and SOA-to-SOA variable optical attenuation. The experimental observations are well correlated to the model analysis of up to four devices interconnected with

variable SOA-to-SOA signal attenuation. The setup of N serial cascaded QW SOAs is shown to achieve novel delay-bandwidth and frequency-tuning characteristics by means of electrical or optical controls and by the number of SOAs coupled by variable SOA-to-SOA attenuation.

The variable optical delay is measured using the experiment for a single device shown in Fig. 1. However, the single QW SOA in this case is replaced by N cascade of QW SOAs schematically shown in Fig. 5. Each QW SOA is 2 mm in length with more than 25-dB gain (at 460 mA) and is controlled by DC controllers, $I_1, I_2, \cdots, I_N$. A given amplifier couples the pump and probe to the next amplifier in cascade with a fixed waveguide-to-fiber loss and variable loss (controlled by experiment). These two losses together are considered as a single variable optical attenuation (VOA). The signal input to the n-th SOA is an output power from the SOA proceeding it. This power is attenuated by the VOA. Therefore, the power input $P_{\mathrm{in},n+1}$ into the $n+1$ amplifier is

$$P_{\mathrm{in},n+1} = \frac{P_{\mathrm{out},n}}{P_{\mathrm{VOA}}} = \frac{P_{\mathrm{out},n}}{10^{P_{\mathrm{VOA}}(\mathrm{dB})/10}}. \quad (3)$$

Considering the above input-output relation and using the probe gain and phase[19,20] for the n-th amplifier in the chain, one obtains the expressions for the total probe gain and phase shift,

$$G = \exp(\sum_{n=1}^{N} G_n L_n), \quad (4)$$

$$\Delta\phi = \sum_{n=1}^{N} \Delta\phi_n. \quad (5)$$

The model of relative phase shift for $N = 1$, $N = 2$, and $N = 4$ cascade with uniformly increasing VOA from 0 dB up to 20 dB is shown in Fig. 6. In the model, the $N = 1$ case and its output power is subsequently used with a varying VOA for the solution of multiple N cascade. Thus, the $N = 1$ response is constant with any variations in VOA. The increase of N (from $N = 2$ to $N = 4$) shows the effect of maximum phase broadening in the frequency domain. At low attenuation (0 dB), the subsequent amplifiers in the cascade are saturated due to the large input power. This successive large optical power broadens the phase spectrum and reduces the maximum phase. As the attenuation is increased, the phase shift is maximized such that each amplifier in cascade is efficiently used for fast-light control. Further increase in optical attenuation results in a reduced fast-light response because of previously presented optical control.

Figure 7 shows the experiment (symbols) and model (lines) of the RF phase (left) and delay-bandwidth product (right) versus VOA for up to $N = 4$ cascaded QW SOAs. The data and model are shown for RF modulation at 1 GHz. The theoretical plots are based on the

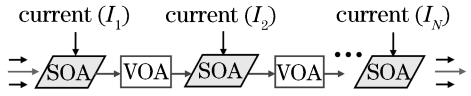

Fig. 5. Schematic of N serially cascaded QW SOAs.

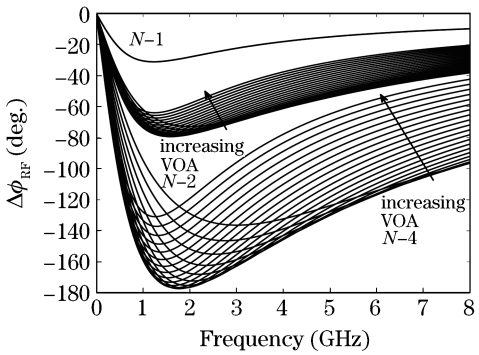

Fig. 6. Model of relative phase shift for $N = 1$, $N = 2$, and $N = 4$ cascaded system with an increasing number of VOAs. The VOA is uniformly increased from 0 to 20 dB. The maximum phase broadening in the frequency domain for larger N cascade is observed.

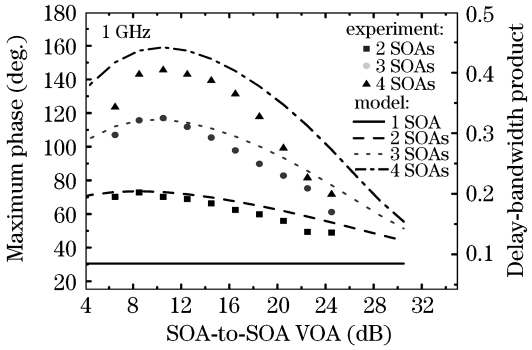

Fig. 7. Experiment (symbols) and model (lines) of maximum RF phase (left) and delay-bandwidth product (right) versus VOA for up to $N = 4$ cascaded QW SOAs.

saturated response of the single QW SOA at about 30° phase change (solid line of $N = 1$ model). The discrepancy of the model from the experiment has the following origins. At a low attenuation and an increased number of SOAs, single-pass lasing occurs, which creates discrepancy in the measured phase. The discrepancy at increased attenuation and increased N is due to phase instability of VOAs at large attenuation settings. The model predicts well the fast-light behavior of our cascaded QW SOAs.

This room-temperature, electrically/optically controlled, fast-light scheme utilizing FWM and CPO in the gain regime of cascaded QW SOAs presents novel bandwidth and phase delay tuning. Experimental relative phase shift of about 160° at 1 GHz (delay-bandwidth product of 0.45) for $N = 4$ QW SOAs is observed. Our theoretical model for N-cascade configuration accurately predicts the scaling behavior with N and SOA-to-SOA VOA coupling.

7. CPO and FWM in QD SOA

The three-dimensional carrier confinement in QDs can be used for slow- and fast-light application to possibly outperform the less-confinement devices. The theoretical investigation for a variable optical buffer in semiconductor QDs has been studied[22]. For the relatively uniform size of a QD ensemble, the density of states becomes narrower, which leads to a higher peak value compared with those of the bulk and QW structures. This also

results in the higher differential gain with a lower carrier injection and can offer a large tunable range of slow- and fast-light devices. In this section, we report the slow and fast light in QD SOA using CPO and FWM.

The InAs QD samples are grown on a nominally exact InP (100) substrates by using metal-organic chemical vapor deposition. The round, dome-shaped QDs with a diameter of around 32 nm and a height of 3.4 nm have been observed by the atomic force microscopic image[23]. The QD density is as high as 1.1×10^{11} cm^{-2}. The processed QD SOAs have a waveguide with seven stacks of QD layers with an InGaAsP barrier of 30 nm[24]. The QD SOAs are fabricated in a 7°-tilted ridge waveguide structure to suppress the reflection at the facets. The intrinsic material loss of the waveguide is 5 cm^{-1}, and the device length of the QD SOA is 1.95 mm.

The RF optical gain spectra as a function of the modulation frequency under different QD SOA injection currents are shown in Fig. 8. The solid curves are based on the theoretical model derived in the previous work[19]. The dotted symbols are experimental data. The modal gains and carrier lifetimes used in the theoretical model are shown in Table 2. Below the transparency current 164 mA, the absorption spectra exhibit the absorption reduction at low modulation frequencies. Above the transparency current, gain spectra show the gain reduction at low modulation frequencies as well. These are due to the carrier beating from the pump and probe interaction. The spectral reductions are more dominant when the QD SOA is biased in high-gain or high-absorption regime. Around the gain transparency current, the RF optical gains are almost constant because fewer electronic transitions or electron beating occur in these regimes. When the QD SOA is changed from the absorption regime to the gain regime, the slope of the refractive index dispersion due to the spectral reduction changes the sign from positive to negative, corresponding to a transition from slow light to fast light[12].

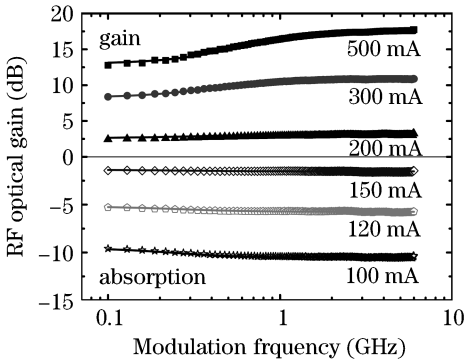

Fig. 8. RF optical gain as a function of the modulation frequency under different current injections into the QD SOA. The solid curves are from theoretical model. The dotted symbols are from the experimental data. The transparency current is 164 mA.

Table 2. Parameters Used in the Calculations of Solid Curves in Figs. 8 and 9

Bias Current (mA)	100	120	150	200	300	500
Modal Gain (cm^{-1})	−13.9	−6.0	−2.0	4.4	17.1	30.5
Carrier Lifetime (ns)	0.80	0.73	0.68	0.60	0.53	0.42

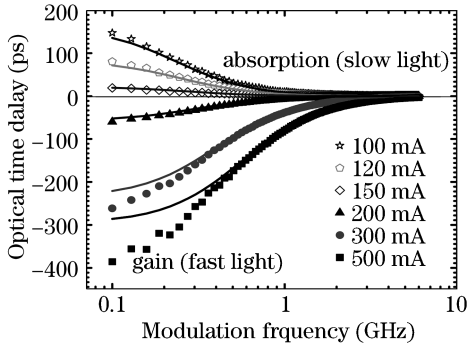

Fig. 9. Optical time delay as a function of the modulation frequency under different current injections into the QD SOA. The solid curves are from the theoretical model. The dotted symbols are from the experimental data. The transparency current is 164 mA.

Figure 9 shows optical time delay as a function of the modulation frequency under different SOA bias currents. As the QD SOA is switched from the absorption regime to the gain regime, switch from slow light to fast light is observed. Thus, we can continuously vary the optical time delay by changing the injection current into the QD SOA. From 100 to 500 mA, the maximum time delay of 533 ps is observed at an 100-MHz modulation. The magnitudes of the time delay become smaller at higher modulation frequencies because carrier beating cannot effectively oscillate at the higher modulation frequencies. Note that the bandwidth of the time delay increases as the operation regime is changed from absorption to the gain. As more carriers are injected into the active region, the carrier lifetime generally decreases due to the stronger electron interactions, as shown in Table 2. Thus, the bandwidth of time delay, which is inversely proportional to the interband carrier lifetime, strongly depends on the bias condition.

The gain spectrum of this QD SOA sample shows a ground-state transition around 1560 nm and an excited-state transition around 1530 nm[15]. As the current injection into the device increases, the modal gain of the ground state saturates more quickly than that of the excited state, as shown in the right axis of Fig. 10. This indicates that the excited state transition has a larger density of states, possibly from the degeneracy. The left axis of Fig. 10 shows the phase shifts of 1.0 GHz

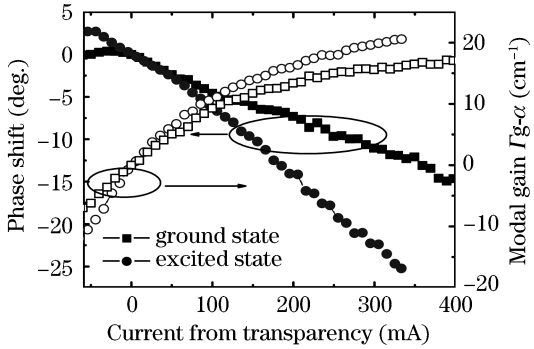

Fig. 10. Comparison between the ground-state and the first-excited-state transitions for phase shift with a modulation frequency of 1 GHz (left axis) and the small signal modal gain (right axis) as a function of the injection current from the transparency current.

modulated signal for the pump energy at the ground-state transition and the excited-state transition. The excited-state transition gives almost twice as much as phase shift compared with that of the ground-state transition. This is mainly due to the higher differential gain of the excited state, and the same trend is observed from the simulations based on the theoretical model. For QDs with reduced inhomogeneous broadening, the differential gain is expected to be much higher than that of the bulk or QW devices due to the delta-like density of states. This experimental relation between the phase shift and the differential gain suggests that with the advancement of the uniform QD growth technology, QD SOAs will be able to achieve more significant slow and fast light compared with those of the bulk or QW SOA due to the possible higher differential gain.

8. Conclusion

In summary, we demonstrated room-temperature, electrically and optically controllable, slow and fast light by means of CPO and FWM in QW and QD SOAs.

First, fast light in QW SOAs has been investigated experimentally and modeled theoretically. The variability of fast light is achieved electrically by changing the background gain using current injection or optically changing the intensity of the input pump power. The study reported a delay of about 80 ps with the bandwidth exceeding 1 GHz using a single QW SOA.

Moreover, a fast-light system of cascaded multiple QW SOAs was investigated. The phase broadening of the coupled system was studied and found to depend on N and VOA coupling. Moreover, the cascaded system explored a behavior of delay-bandwidth product with N. Under maximized VOA coupling and input power, the delay-bandwidth product was shown to linearly scale with the number N of QW SOAs. The delay-bandwidth product was shown to be optically controllable with SOA-to-SOA VOA. The experimental measurements of up to four cascaded QW SOAs agree with theoretical predictions.

Finally, we investigated slow and fast light in the QD SOA by absorption-to-gain switching in the QD SOA. A larger tunable phase shift has been observed at the excited-state transition than that at the ground-state transition due to the larger differential gain. With advancement of QD growth and processing technologies and, therefore, enhanced device gains, the CPO/FWM slow- and fast-light effects should result in substantial tunable optical delays using QD SOAs.

We thank Professor Connie Chang-Hasnain at University of California at Berkeley, USA, and Professor Hailin Wang at University of Oregon, USA, for technical discussions. We also thank Dr. Hui Su at Emcore, CA, USA, Professor Donghan Lee at Chungnan National University, South Korea, and Professor Weonguk Jeong at Sungkyunkwan University, South Korea, for previous collaborations during this research. This work was supported by DARPA Slow Light Program. Shun Lien Chuang is the author to whom the correspondence should be addressed, his e-mail address is s-chuang@uiuc.edu.

References

1. H. Toda, F. Nakada, M. Suzuki, and A. Hasegawa, IEEE Photon. Technol. Lett. **12,** 708 (2000).
2. L. V. Hau, S. E. Harris, Z. Dutton, and C. H. Behroozi, Nature **397,** 594 (1999).
3. M. S. Bigelow, N. N. Lepeshkin, and R. W. Boyd, Phys. Rev. Lett. **90,** 113903 (2003).
4. P. C. Ku, F. Sedgwick, C. J. Chang-Hasnain, P. Palinginis, T. Li, H. Wang, S. W. Chang, and S. L. Chuang, Opt. Lett. **29,** 2291 (2004).
5. H. Takahashi, P. Carlsson, K. Nishimura, and M. Usami, IEEE Photon. Technol. Lett. **16,** 2063 (2004).
6. Y. Sugimoto, S. Lan, S. Nishikawa, N. Ikeda, H. Ishikawa, and K. Asakawa, Appl. Phys. Lett. **81,** 1946 (2002).
7. H. Su and S. L. Chuang, Opt. Lett. **31,** 271 (2006).
8. H. Su and S. L. Chuang, Appl. Phys. Lett. **88,** 061102 (2006).
9. M. van der Poel, J. Mørk, and J. M. Hvam, Opt. Express **13,** 8032 (2005).
10. J. Mørk, R. Kjaer, M. van der Poel, and K. Yvind, Opt. Express **13,** 8136 (2005).
11. S. W. Chang, P. K. Kondratko, H. Su, Member, and S. L. Chuang, IEEE J. Quantum Electron. **43,** 196 (2007).
12. P. K. Kondratko and S. L. Chuang, Opt. Express **15,** 9963 (2007).
13. P. K. Kondratko, S. W. Chang, H. Su, and S. L. Chuang, Appl. Phys. Lett. **90,** 251108 (2007).
14. F. Ohman, K. Yvind, and J. Mørk, Opt. Express **14,** 9955 (2006).
15. A. Matsudaira, D. Lee, P. Kondratko, D. Nielsen, S. L. Chuang, N. J. Kim, J. M. Oh, S. H. Pyun, W. G. Jeong, and J. W. Jang, Opt. Lett. **32,** 2894 (2007).
16. F. Ohman, K. Yvind, and J. Mørk, IEEE Photon. Technol. Lett. **19,** 1145 (2007).
17. P. Agrawal, J. Opt. Soc. Am. B **5,** 147 (1988).
18. B. Pesala, Z. Y. Chen, A. V. Uskov, and C. J. Chang-Hasnain, Opt. Express **14,** 12968 (2006).
19. H. Su, P. Kondratko, and S. L. Chuang, Opt. Express **14,** 4800 (2006).
20. P. K. Kondratko, "Slow and fast light using quantum-dot and quantum-well semiconductor optical amplifiers" Ph. D. Thesis (University of Illinois at Urbana-Champaign 2007).
21. G. Eisenstein, N. Tessler, U. Koren, J. M. Wiesenfeld, G. Raybon, and C. A. Burrus, IEEE Photon. Technol. Lett. **2,** 790 (1990).
22. C. J. Chang-Hasnain, P. C. Ku, J. Kim, and S. L. Chuang, Proc. IEEE **91,** 1884 (2003).
23. N. J. Kim, J. M. Oh, D. Lee, S. H. Pyun, D. G. Ko, J. H. Yoon, W. G. Jeong, and J. W. Jang, Appl. Phys. Lett. **90,** 241108 (2007).
24. H. D. Kim., W. G. Jeong, J. H. Lee, J. S. Yim, D. Lee, R. Stevenson, P. D. Dapkus, J. W. Jang, and S. H. Pyun, Appl. Phys. Lett. **87,** 083110 (2005).